# Synthesis, Characterization and Optical Properties of Ni-Doped Tin Oxide

Syed Zafar Ilyas[1], M. Asghar[2], Mahwish Anwer[1] and Ghulam Nabi[3]

1. *Department of Physics Allama Iqbal Open University (AIOU), Islamabad, Pakistan*
2. *Department of Physics, IU, Bahawalpur, Pakistan*
3. *Department of Physics, University of Gujrat, Hafiz Hayat Campus, Gujrat 50700, Pakistan*

* **Corresponding Author**: Email: mhashmi@iub.edu.pk

## Abstract

*A systematic study on the preparation of pure $SnO_2$ nano-particles and Ni-doped $SnO_2$ with different doped concentrations (0%, 0.3%, 0.7%) have been conducted. Facile sol-gel technique has been used for sample preparations where as $SnCl_4$, $NiCl_2$ and ammonia solutions were used as precursors. The influence of the Ni doping concentration on the structure and optical properties of synthesized samples of $SnO_2$ was investigated. Pure and Ni doped $SnO_2$ nano-particles have been characterized by using X-rays diffraction (XRD), scanning electron microscopy (SEM), U.V and photoluminescence spectroscopy. X-ray diffraction patterns showed for all samples that $SnO_2$ have tetragonal structure with no additional peaks corresponding to parasitic phases. This showed that doped material has been accommodated uniformly inside the $SnO_2$. Particles size of pure and Ni doped nano-particles was calculated and has ranged from 4 nm to 25 nm. An increasing behaviour of particles size has been observed with increasing percentage of Ni. Optical properties of the pure and doped materials showed that decreasing behaviour of optical energy band gap with increasing concentration of Ni which revealed that the nanometric size of the materials influences the energy band gap values. Optical transmittance was also measured at room temperature which showed an increasing behaviour with increasing doping concentration.*

**Key Words:** $SnO_2$; Ni doping; Nano-particles; Sol-Gel Method; Optical Properties.

## 1. Introduction

Nano particles have acquired a great importance in the field of research on the behalf of their distinctive physical, chemical, magnetic and optical properties. Nanoparticles show superiority over bulk material due to their mechanical strength, thermal stability, catalytic activity, electrical conductivity, magnetic properties and optical properties. Tin oxide nanoparticles were used as a gas sensing material for manufacturing of gas sensors devices, transparent conducting electrodes, photochemical and photoconductive devices and gas discharge display bring a great development in the field of Nano-science. More over optical properties of tin oxide changes with nanoparticles size that are being useful for optoelectronics devices like solar cell, lithium rechargeable batteries and photoconductor [1-6]. Tin oxide is n-type semiconductor whose reported band gap was found to be 3.6-3.8eV [7]. Sol-gel, hydrothermal method [8], precipitation, carbo thermal reduction, polymeric precursor and thin film by chemical vapor deposition [9] are commonly used different techniques to prepare $SnO_2$. In present research work sol-gel method was adopted for the synthesis of pure $SnO_2$ and Ni doped $SnO_2$.

## 2. Materials and Methods

The chemicals used in this work were tin (IV) chloride, tetra hydrate ($SnCl_4$), ammonium hydroxide, ($NH_4OH$ 31%), $NiCl_2$ and ultra-pure water.

### Synthesis of Ni Doped $SnO_2$ Nanoparticles

Dissolve 2.6ml of $SnCl_4$ in 41ml of distilled water. After adding impurity ($NiCl_2$), solution is positioned on magnetic stirrer for 20 minutes. Ammonia solution about 20ml falls drop wise through pipit, in solution under perpetual stirring. Dropping rate of ammonia is well controlled during the experiment. This solution is stirred again for 2hr. After this sol was formed as shown in fig 1 aged at refrigerator for 15min. The sol was converted into gel. The gel was dried at $100^0$C. After drying it is crushed into powder. The resulting powder annealed at 350$^o$C for one hour. Finally Nickel doped tin oxide was obtained.

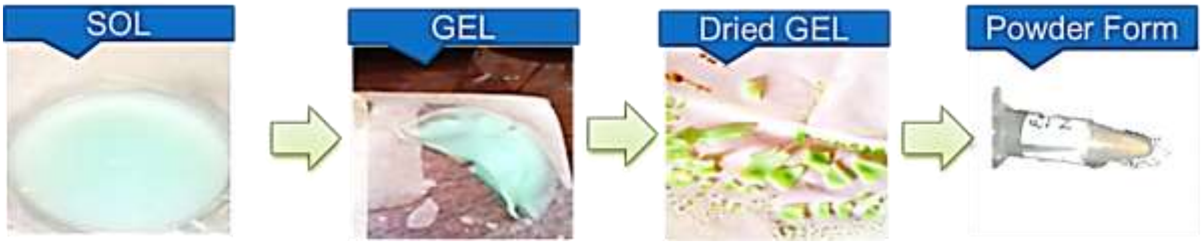


**Figure. 1:** Synthesis of Ni-doped tin oxide

## 3. Results & Discussion

### XRD

X-ray diffraction patterns were obtained for calcined pure $SnO_2$ and Ni doped $SnO_2$ using $CuK_\alpha$ radiation of wavelength 1.54060 Å with scanning time 0.2500s. The samples were scanned between 20-80° 2θ angles. The diffraction peaks obtained in the XRD patterns counterparts with a pure XRD pattern that are in good agreement with standard values as recorded in the JCPDS Card (01-077-0447) shown in fig. 1-3. The tetragonal structure of $SnO_2$ does not change by the Ni doping. It was observed that the intensity of peaks decreases with increasing concentration of Ni and there is increment increased observed in full width at half-maximum (FWHM) widths of the peaks which indicated that the particles size of the Ni doped $SnO_2$ powders decrease as the Ni concentration increases. It also observed that when the concentration of Ni sudden increases then the intensity of XRD increase, and the full width half-maximum (FWHM) widths of the peaks decrease indicates that the crystallite size of the Ni doped $SnO_2$ powders become increase as the sudden increase Ni concentration. It is also observed that the peak positions XRD spectra, does not change which specify the rutile structure remains the same on sudden increase in Ni concentration. Debye-Scherer formula equation (1) is used to determine the particles size [10-11].

$$D = \frac{0.9\lambda}{\beta Cos\Theta} \quad (1)$$

Where wavelength of X-Ray (0.1541nm) shown by 'λ', FWHM (full width at half maximum) is shown by 'β', diffraction angle shown by 'ɵ' and particle diameter size is shown by 'D'.

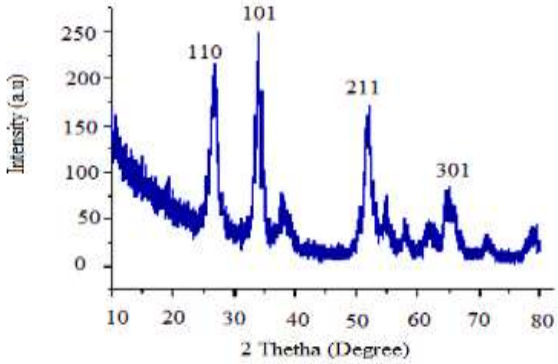


**Figure. 2:** XRD Pattern for pure tin oxide

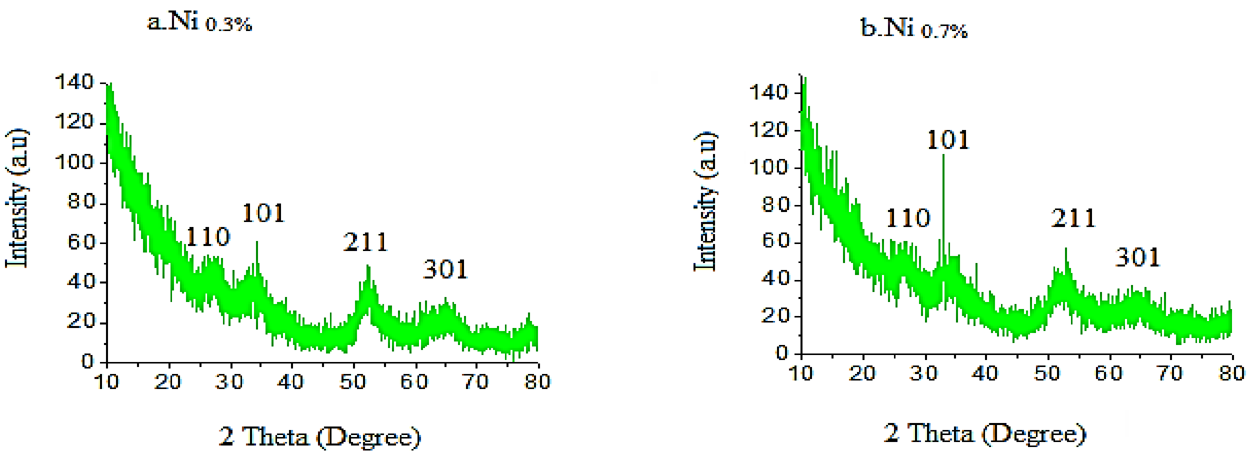


**Figure. 3:** XRD pattern of Ni-doped tin oxide for different % of doping

**Table 1:** Calculated particle size of pure and Ni-doped $SnO_2$

| Sr. No. | Sample Type | Doping Mass %age | Analyses Peak | FWHM | Particle Size |
|---|---|---|---|---|---|
| 1 | So | Pure tin oxide 0% | $34^0$ | 0.6298 | 12.3nm |
| 2 | S1 | Doped with Ni 0.3% | $34^0$ | 1.8893 | 4.01nm |
| 3 | S2 | Doped with Ni 0.7% | $34^0$ | 0.1181 | 65.5nm |

## SEM

SEM images shown in fig. 4-5 revealed that Ni doped tin oxide has tetragonal rutile structure. Doping concentration does not change the morphology of the pure tin oxide, but the particle size get change. The average size from SEM was measured to 10 to 300 micrometre**.**

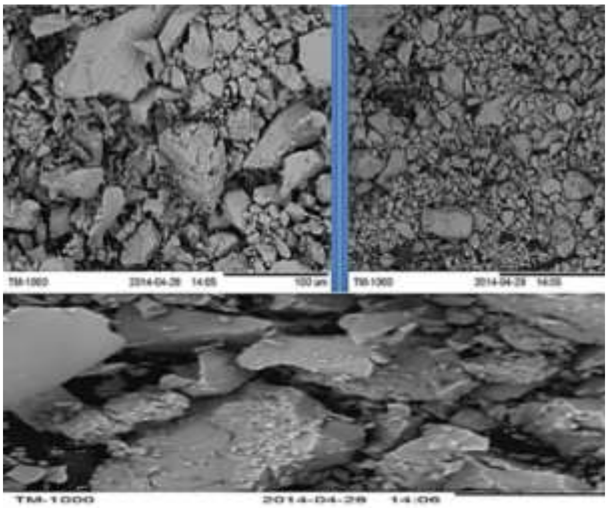

**Figure. 4:** SEM images of Ni $_{0.3}$ doped tin oxide

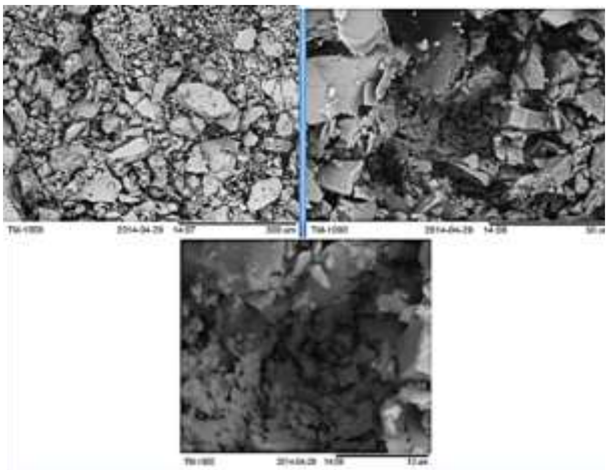

**Figure. 5:** SEM images of Ni $_{0.7}$ doped tin oxide

## U.V Spectrophotometer

The extrapolating straight line in the graph of $(\alpha h\nu)^2$ vs bandgap (eV) shown in fig. 7 the measured value of the band gap for Ni doped tin oxide which was also confirmed by PL spectra. The observation of U.V spectra shown in fig. 6 reveals that the optical transmittance of Ni doped tin oxide depends on wavelength. In a visible region the transmittance of these particles is high over a wide range. Around 100% transmittance was observed for Ni doped $SnO_2$, which has ranged from 300 nm to 800 nm [11].

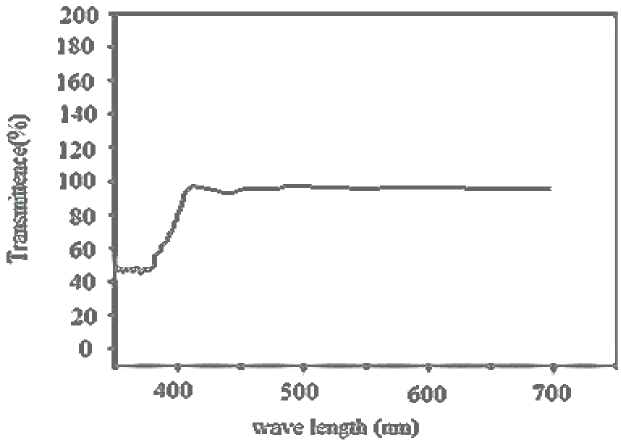


**Figure. 6:** U.V Spectrum for Ni-doped tin oxide

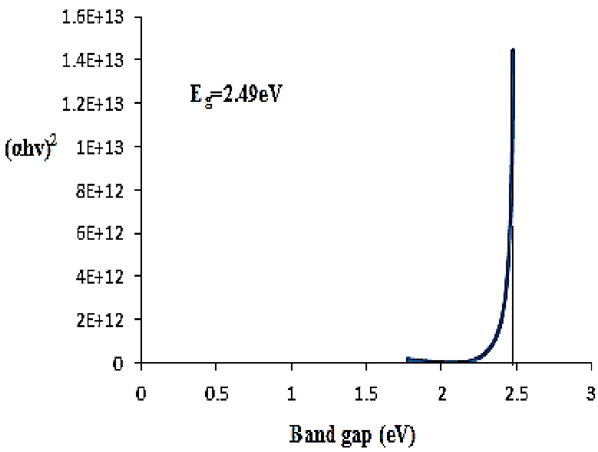


**Figure. 7:** Band gap for Ni-doped tin oxide

## Photoluminescence Spectroscopy

PL spectra show the relation among intensity and wavelength. Tauc relation was used to measure the band gap [12]. The calculated values of Eg for

$SnO_2$ are set up to be about 3.78 eV that is approximately equal to the previous reported work [13].The calculated value of band gap for Ni-doped tin oxide at wavelength of 500nm is 2.47eV. When the doping concentration increases then the peak observed at 455nm and band gap was found to be 2.72eV. It was observed tin oxide doped with different concentration of Ni, then peak shifted at different wavelength due to which the band gap increases by increasing doping concentration of Ni.

**Table 2:** Eg measured value by PL spectra for pure $SnO_2$

| Sr. No. | Symbol | Name | Value |
|---|---|---|---|
| 1 | $E_g$ | Band gap | 2.47eV |
| 2 | H | Plank constant | $6.62 \times 10^{-34}$ $m^2$ kg/s |
| 3 | C | Speed of light | $3\times10^8$m/s |
| 4 | $\lambda$ | Wave Length | 500nm |

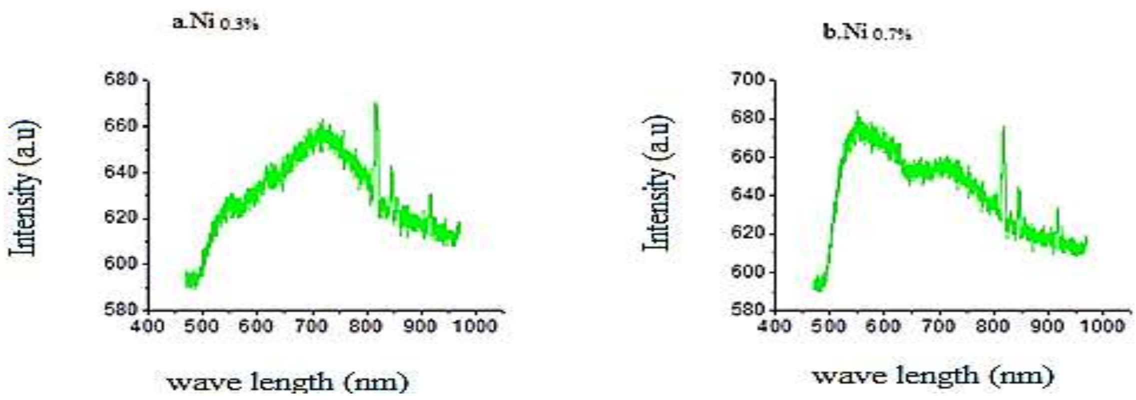


**Figure. 8:** PL spectra for Ni-doped tin oxide

## Conclusion

In present research work synthesize of Ni doped $SnO_2$ nano particles by using sol-gel method was done successfully and characterized the grown samples by changing various parameters like temperature, feeding rate of ammonia solution and doping concentration. SEM image shows the grown nanoparticles of Ni doped $SnO_2$ has tetragonal rutile structure.

XRD data used to calculate the particle size and it is suggested that the doping concentration does not effect on morphology of nano particles, but it changes the particles size.

UV results show that the transmission increases with increasing Ni-doping concentration while PL spectra show the band gap increases with doping concentration.

## References

[1] Kay, A., & Grä tzel, M. (2002). Dye-sensitized core−shell nanocrystals: improved efficiency of mesoporous Tin Oxide electrodes coated with a thin layer of an insulating oxide, Chem. Mater., 14, 2930-2953.

[2] Choudhury, S., Betty, C. A., Girija, K. G., & Kulshreshtha, S. K. (2006). Room temperature gas sensitivity of ultrathin $SnO_2$ films prepared from Langmuir-Blodgett film precursors. Appl. Phys. Lett. 89, 071914.

[3] Triantafyllopoulou, R., Illa, X., Casals, O., Chatzandroulis, S., Tsamis, C., Romano-Rodriguez, A., & Morante, J. R. (2008). Nanostructured oxides on porous silicon microhotplates for $NH_3$ sensing. Microelectronic Engineering, 85, 1116-1119.

[4] Liu, H.,.Avrutin, V., Izyumskaya, N.,. Özgür, Ü, & Morkoç H. (2010). Transparent conducting oxides for electrode applications in light emitting and absorbing devices, Superlattices and Microstructures, 48, 458-484.

[5] Patil, G. E., Kajale, D. D., Chavan, D. N., Pawar, N. K., Ahire, P. T., Shinde, S. D., Gaikwad, V. B., & Jain, G. H. (2011). Synthesis, characterization and gas sensing performance of SnO2 thin films prepared by spray pyrolysis. Bulletin of Materials Science, 34, 19.

[6] Kim, C., Noh, M., Choi, M., Cho, J., & Park, B., (2005) Critical size of a nano SnO2 electrode for Li-secondary battery, Chem. Mater. 17, 3297-3301.

[7] Bagheri-Mohagheghi, M. -M.; Shahtahmasebi, N.; Alinejad, M. R.; Youssefi, A.; Shokooh-Saremi, M. (2008) The effect of post-annealing temperature on the nano-structure and energy band gap of $SnO_2$ semiconducting oxide nano-particles synthesized by polymerizing-complexing sol-gel method. Physica B, 403, 2431.

[8] Ibarguen, C. A.; Mosquera, A., Parra, R., Castro, M. S., & Rodríguez-Páez, J. E. (2007). Synthesis of $SnO_2$ nanoparticles through the controlled precipitation route. Mater. Chem. Phys., 101, 433.

[9] Chi, K.-M.; Lin, C.-C.; Lu, Y.-H.; Liao, J.-H. (2000). Chemical vapour deposition of $SnO_2$ thin films from Bis(β-diketonato)tin complexes. J. Chin. Chem.Soc.,47, 425-431.

[10] Nath, S. S., Chakdar, D., and Gope G. (2007). Synthesis of CdS and ZnS quantum dots and their applications in electronics. Nanotrends – A Journal of Nanotechnology and its Applications 02-03.

[11] Hall, B. D., Zanchet, D., & Ugarte, D. (2000).Estimating nanoparticle size from diffraction measurements. J. App. Cryst., 33, 1335-1341.

[12] Pankove, J. I. (1971) Optical Processes in Semiconductors: Englewood Cliffs NJ; Prentice-Hall Inc.

[13] Gnanam, S., & Rajendran, V. (2010). Luminescence properties of eg-assisted $Sno_2$ nanoparticles by Sol-Gel Process. Digest Journal of Nanomaterials and Biostructures, 5, 699-704.